Khaidukov Z.V, Simonov Yu.A.

17.09.2019

Thermodynamics of quark-gluon plasma at finite baryon density.

In this report we will discuss properties of the quark-gluon plasma in the presence of the baryon chemical potential μ_B using the Field Correlator Method. The nonperturbative FCM dynamics includes the Polyakov line, computed via colorelectric string tension $\sigma^E(T)$ and the quark and gluon Debye masses, defined by the colormagnetic string tension $\sigma^H(T)$. The resulting QGP thermodynamics at $\mu_B \leq 400$ MeV is in a good agreement with the available lattice data,both pressure and the sound velocity do not show any sign of a critical behaviour in this region.

Motivation

The main result of heavy ion experiments performed over the last 15 years at RHIC and then at RHIC and LHC is the discovery of a new form of matter with its properties markedly different from the pre-RHIC era

Instead of the commonly assumed picture of weakly coupled Quark-Gluon Plasma(QGP) a strongly coupled liquid has emerged, subject to the law of the relativistic hydrodynamics

Motivation

Another striking discovery was the analysis of the temperature transition, made in the $2 + 1$ QCD lattice computations, which showed a smooth crossover in the temperature region $T = 140 \div 180$ MeV

At this moment one of the main sources of information is the Lattice calculations. The presence of strong interaction in QGP at zero baryon density was demonstrated in numerous studies. They show that the ratio of the QGP pressure to the non-interacting case is less than 0.8 and remains almost constant with increasing temperature.Another striking discovery in this domain was the analysis of the temperature transition, made in the $2 + 1$ QCD lattice computations, which has shown a smooth crossover in the temperature region $T = 140...180$ MeV

Despite such a dramatic progress the question about the structure of the QCD phase diagram at nonzero baryon density remains open. This happens mostly because lattice methods in case of $N_c = 3$ are strongly restricted in the domain of baryon chemical potentials due to the sign

Lattice

To circumvent this difficulty in case of $N_c = 3$ one can use the Taylor expansion around zero chemical potential

Imaginary chemical potential

In both cases strong limitations due to existence of Roberge–Weiss point $\frac{\mu}{T} = \pm i\pi$.

Decrease the number of colours to $N_c = 2$, where the sign problem is absent.

The Field Correlator Method

Field Correlator Method (FCM) is applicable in QCD at any chemical potential and any temperature. In this method the nonperturbative dynamics in confinement and deconfinement regions is based on vacuum properties, described by gluonic field correlators and the key role is played by correlators of colorelectric fields D^E and colormagnetic fields D^H, which provide colorelectric confinement (CEC) with the string tension $\sigma^E(T)$ and colormagnetic confinement (CMC) with the string tension $\sigma^H(T)$. The latter being calculated from field correlators and on the lattice, grows with T , $\sigma^H(T) \sim g^4(T)T^2$ and insures the strong interaction at large T mentioned above.

The Field Correlator Method

At zero temperatures in this model exists confinement(!) thus one can observe formation of the string between colour objects. And one can find masses of all mesons and baryons. We will not investigate this situation in details. Because we will focus on deconfinement domain.

The Field Correlator Method

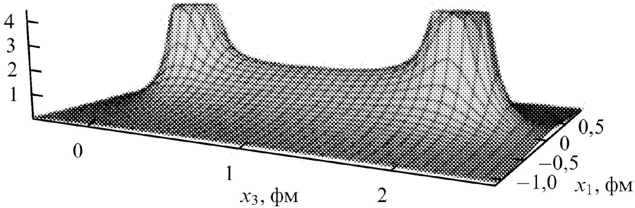

The Field Correlator Method

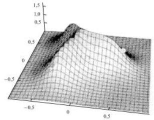

Рис. 15. Распределение поля $\mathcal{E}^{(\mathrm{B})}$ (80), (81) с учетом только вклада коррелятора D в плоскости кварков, образующих равносторонний треугольник со стороной 1 фм. Положения кварков показаны точками.

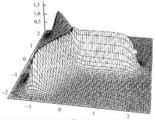

Рис. 16. Распределение поля $\mathcal{E}^{(\mathrm{B})}$ (80), (81) с учетом только вклада коррелятора D в плоскости кварков, образующих равносторонний треугольник со стороной 3,5 фм. Положения кварков показаны точками.

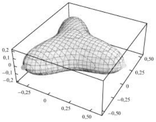

Рис. 17. Поверхность $|\mathcal{E}^{(\mathrm{B})}(\mathbf{x})| = \sigma$ при расстоянии между кварками 1 фм. Положения кварков показаны точками.

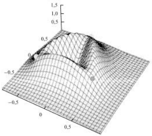

Рис. 18. Распределение поля $|\mathcal{E}_{\Delta}^{(\mathrm{G})}(\mathbf{x})|$ (82) треугольного глюбола в плоскости валентных глюонов, расстояние между которыми 1 фм. Положения валентных глюонов показаны точками.

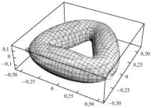

Рис. 19. Поверхность $|\mathcal{E}_{\Delta}^{(\mathrm{G})}(\mathbf{x})| = \sigma$ при расстоянии между валентными глюонами 1 фм. Положения валентных глюонов показаны точками.

рыми 1 фм, а на рис. 19 — поверхность, определяемая условием $|\mathcal{E}_{\Delta}^{(\mathrm{G})}(\mathbf{x})| = \sigma$, для той же конфигурации валентных глюонов с расстоянием друг от друга 1 фм.

Заметим, что согласно (38) статический кварк-антикварковый потенциал можно вычислить как работу, совершаемую при удалении его от антикварка на данное расстояние R. Аналогичное соотношение выполняется для поля и потенциала Δ-глюбола (79), (82). При этом недиагональная часть потенциала в Δ-глюболе V^{nd} равна работе силы, действующей на данный (эффективный) кварк со стороны внешней струны, и связана с интерференцией (наложением) мезонных полей $\mathcal{E}^{\mathrm{M}}$ в окрестностях порядка λ вокруг валентных глюонов.

5. Заключение

В обзоре мы рассмотрели следующие вопросы: вакуумные поля в КХД, механизм конфайнмента, образование струны КХД и, наконец, распределение полей внутри адронов.

The Field Correlator Method

In the FCM at finite temperatures the basic interaction of a quark or a gluon can be expressed via world lines affected by the vacuum fields and finally written in the form of Wilson loops and Polyakov lines. It is essential that in the deconfined phase two basic interactions define quark and gluon dynamics: the colorelectric (CE) interaction, contained in the Polyakov line L(T), and the colormagnetic (CM) one in the spatial projection on the Wilson loop.

The Field Correlator Method

Using the T dependent path integral (world line) formalism one can express thermodynamic potentials via the Wilson loop integral, e.g. for the gluon pressure one has

$$P_{gl} = 2(N_c^2 - 1) \int_0^\infty \frac{ds}{s} \sum_{n=1,2..} G^n(s) \tag{1}$$

s-proper time, and for $G^n(s)$ one can obtain:

$$G^n(s) = \int (Dz)^{\omega}_{on} exp(-K) \hat{tr}_a < W^a_\Sigma(C_n) > \tag{2}$$

where $K = \frac{1}{4} \int_0^s d\tau (\frac{dz^\mu}{d\tau})^2$, and $W^a_\Sigma(C_n)$ is the adjoint Wilson loop defined for the gluon path C_n, which has both temporal (i4) and spacial projections (ij), and $\hat{tr}_a$ is the normalized adjoint trace.

The Field Correlator Method

When $T > T_c$ the correlation function between CE and CM fields is rather week

$$< E_i(x) B_k(y) \Phi(x, y) \approx 0 \quad (3)$$

The expression for the Wilson loops is factorized

$$< W_\Sigma^a(C_n) >= L_{adj}^{(n)}(T) < W_3 > \quad (4)$$

with $L_{adj}^{(n)} \approx L_{adj}^n$ for $T \leq 1$ GeV.

The Field Correlator Method

One can integrate out the z_4 part of the path integral $(Dz)^{\omega}_{on} = (Dz_4)^{\omega}_{on} D^3 z$, with the result

$$G^{(n)}(s) = G_4^{(n)}(s) G_3(s) \tag{5}$$

$$G_4^n(s) = \int (Dz_4)^{\omega}_{on} e^{-K} L^{(n)}_{adj} = \frac{1}{2\sqrt{4\pi s}} e^{-\frac{n^2}{4T^2 s}} L^{(n)}_{adj} \tag{6}$$

This factorization holds also for quarks and will be used below (changing the adjoint representation for the fundamental one)

The Field Correlator Method

The resulting gluon contribution is

$$P_{gl} = \frac{N_c^2 - 1}{\sqrt{4\pi}} \int_0^\infty \frac{ds}{s^{3/2}} G_3(s) \sum_{n=0,1,2,\dots} e^{-\frac{n^2}{4T^2 s}} L_{adj}^n, \qquad (7)$$

$$G_3(s) = \int (D^3 z)_{xx} e^{-K_{3d}} < \hat{tr}_a W_3^a > \qquad (8)$$

To account for CMC one can introduce an approximate expression for 3d Green function

$$G_3(s) = \frac{1}{(4\pi s)^{3/2}} \sqrt{\frac{(M_{adj}^2)s}{sinh(M_{adj}^2)s}}, M_{adj} \approx 2M_D \qquad (9)$$

where M_D is the gluon Debye mass that emerges via magnetic string

The Field Correlator Method

The full pressure reads as:

$$P_{tot} = P_f + P_{gl} \tag{10}$$

One can see that the expression should be analytically continued for high densities. We use the form:

$$\frac{P_q(T,\mu)}{T^4} = f_+(T,\mu) + f_-(T,\mu), \tag{11}$$

$$f_\pm(T,\mu) = \frac{N_c}{3\pi^2}\int_0^\infty \frac{dz\left(z^2 + 2z\frac{\bar{M}}{T}\right)^{3/2}}{1 + \exp\left(z + \frac{\bar{M}}{T} + \frac{V_1(T)}{2T} \mp \frac{\mu}{T}\right)}, \tag{12}$$

The Field Correlator Method

Analytical study of our equations needs some efforts. But one can see that in this formalism we obtained Roberge–Weiss point $\frac{\mu}{T} = \pm i\pi$, due to the vanishing of denominator in the equation for the pressure

Two limits are simply done,one is the Stefan-Boltzman limit at high T and another is the free quark limit with M tends to m_q and $V_1 = 0 (L = 1)$ at extremely low temperatures, at this conditions the Fermi sphere is forming .

Polyakov line calculations.

One of the ways to calculate L is to evaluate it via the heavy-light mass M_{HL}. The mass $M_{HL}(T)$,which is T-dependent due to the temperature dependent string tension $\sigma^E(T)$ with the relation $M_{HL}(T) \sim \sqrt{\sigma^E(T)}$. To find $\sigma^E(T)$ explicitly one can use a connection between σ^E and the quark condensate $\bar{q}q$

We take the CE string tension in the massless quark limit related to the chiral condensate as $|\bar{q}q(T)| = const(\sigma(T))^{3/2}$. Introducing a dimensionless parameter $a(T)$ as $\sigma(T) = \sigma(0)a^2(T)$, one has

$$|\bar{q}q(T)| = |\bar{q}q(0)|a^3(T) \qquad (13)$$

.

As a result one has $M_{HL}(T) = M_{HL}(T_0)\frac{a(T)}{a(T_0)}$ and $L(T) = \exp\left(-\frac{M_{HL}(T)}{T}\right)$

Polyakov line calculations.

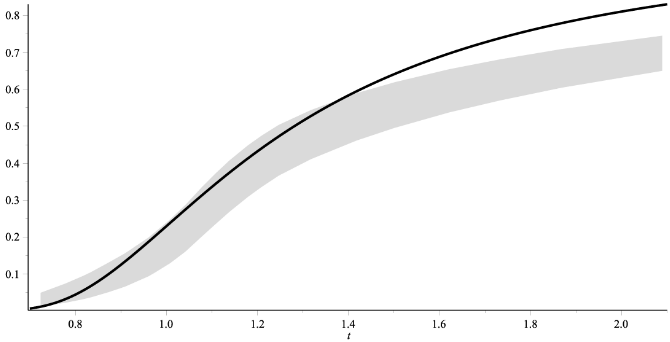

Figure: The Polyakov line as a function of $t = T/T_c, T_c$=160 MeV.Grey band corresponds to L_{HL} within the accuracy limits of a(T). The solid black line is the " ideal" L_{FCM}

Pressure at zero baryon chemical potentials

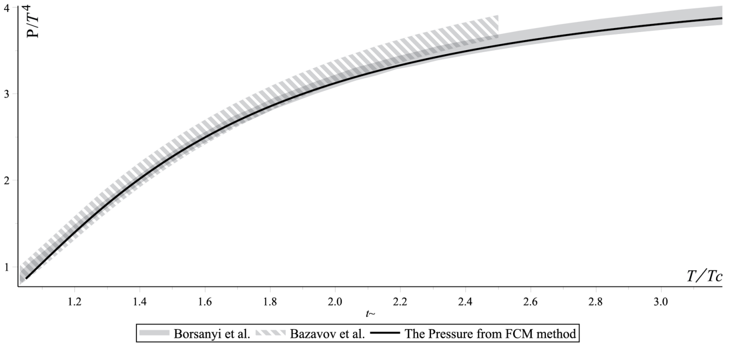

Figure: The QGP pressure as a function of T/T_c. The grey band is the lattice data of Borsanyi et al. and the striped band is the lattice data from Bazavov et al.

Scale anomaly.

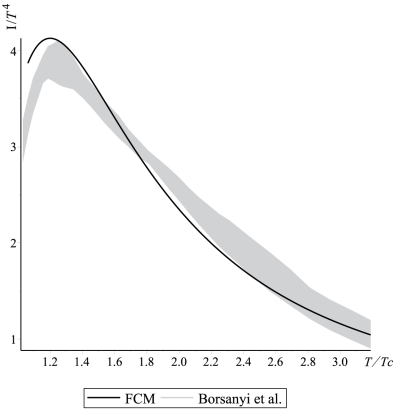

Figure: The anomaly in QGP as a function of T/T_c. The grey band is the lattice data of Borsanyi et al.

Pressure at finite baryon chemical potential.

To test ourselves we have calculated the pressure at $\mu_B = 100, 200, 300$ MeV and μ_B=400 MeV.

Pressure at finite baryon chemical potential.

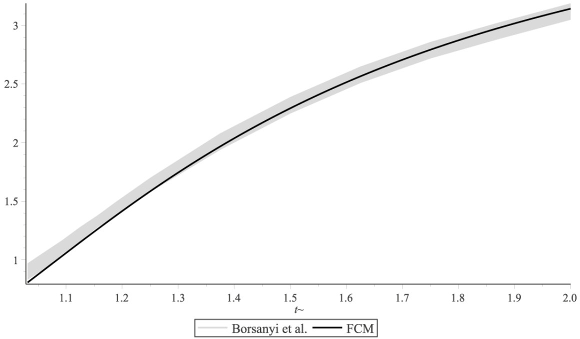

Figure: The QGP pressure as a function of T/T_c for $\mu_B = 100$ MeV . The grey band is the lattice data of Borsanyi et al.

Pressure at finite baryon chemical potential.

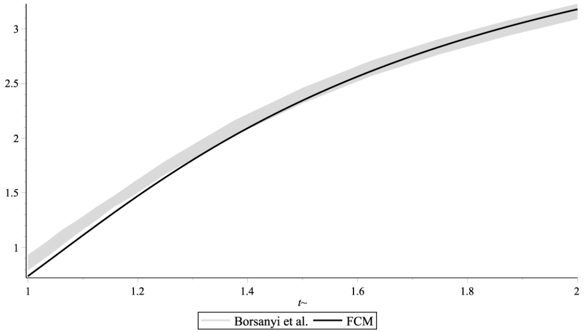

Figure: The QGP pressure as a function of T/T_c for $\mu_B = 200$ MeV . The grey band is the lattice data of Borsanyi et al.

Pressure at finite baryon chemical potential.

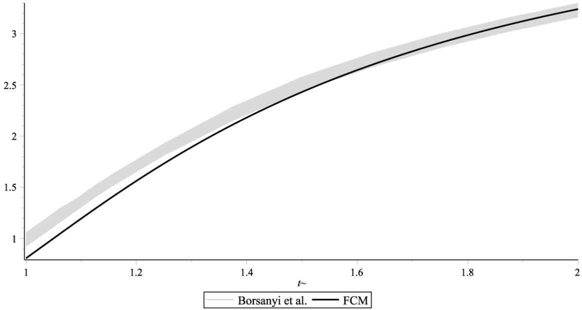

Figure: The QGP pressure as a function of T/T_c for $\mu_B = 300$ MeV . The grey band is the lattice data of Borsanyi et al.

Pressure at finite baryon chemical potential.

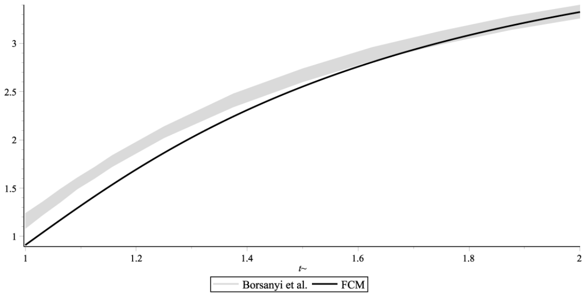

Figure: The QGP pressure as a function of T/T_c for $\mu_B = 400$ MeV . The grey band is the lattice data of Borsanyi et al.

Pressure at finite baryon chemical potential.

As one can see from the last figure,at sufficiently high baryon densities the disagreement with the lattice data becomes stronger. One can improve this situation taking into account the renormaliztion of Polaykov line with densities

Pressure at finite baryon chemical potential.

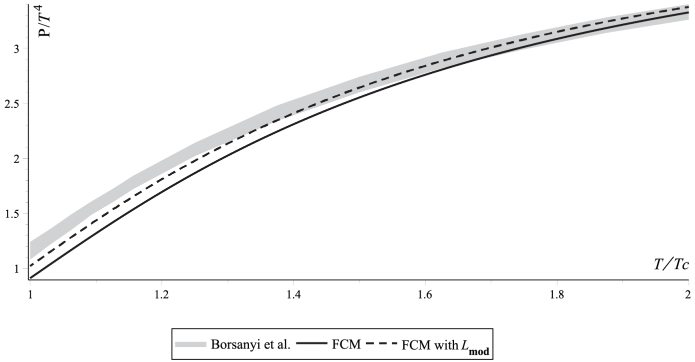

Figure: The ratio of QGP pressure to T^4 as a function of T/T_c for $\mu_B = 400$ MeV with L_{FCM}(black line) and with Polyakov line that is scaled ,similar to PhysRevD.76.114509 (dashed line) .

Pressure at finite baryon chemical potential.

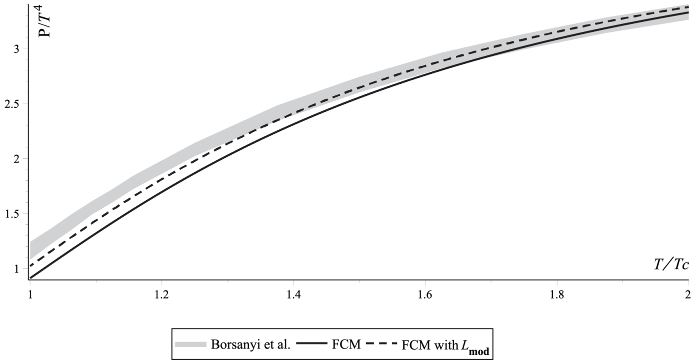

Figure: The ratio of QGP pressure to T^4 as a function of T/T_c for $\mu_B = 400$ MeV with L_{FCM}(black line) and with Polyakov line that is scaled ,similar to PhysRevD.76.114509 (dashed line) .

Speed of sound at finite baryon density.

There are several possibilities to define the speed of sound at nonzero μ , and we will focus on the isoentropic definition i.e $s/n = \text{const}$:

$$C_s^2 = \frac{n^2 \frac{\partial^2 P}{\partial T^2} - 2sn \frac{\partial^2 P}{\partial T \partial \mu} + s^2 \frac{\partial^2 P}{\partial \mu^2}}{(\varepsilon + p)\left(\frac{\partial^2 P}{\partial T^2}\frac{\partial^2 P}{\partial \mu^2} - \left(\frac{\partial^2 P}{\partial T \partial \mu}\right)^2\right)} = \frac{1}{\kappa_s(\epsilon + p)}, \tag{14}$$

where we have defined:

$$s = \frac{\partial P}{\partial T}, \quad n = \frac{\partial P}{\partial \mu}, \quad \varepsilon + P = Ts + \mu n. \tag{15}$$

The square of the speed of sound at finite baryon density.

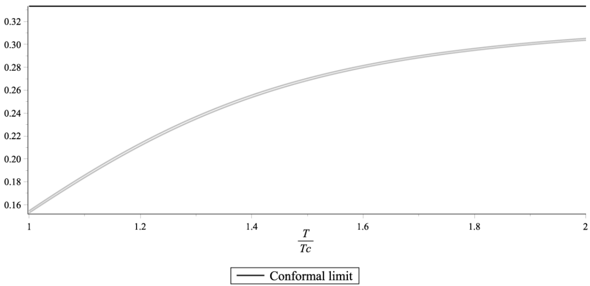

Figure: The width of solid the line is the changing of the speed of sound in the range $\mu_B = 0..300 MeV$

Conclusions and discussions

We have exploited above the FCM thermodynamics to calculate the QGP pressure at finite baryon density in the temperature range $1 < T/T_c < 2$ Our basic dynamics was defined by two factors; the Polyakov line that is connected with $L_{HL}(T) = \exp(-M_{HL}/T)$, and the colormagnetic confinement (CMC) in the exponential form with the CMC quark mass $M_D = c\sqrt{\sigma^H(T)}$, where $c = 1.6$.
We have demonstrated that the resulting pressure $P_{FCM}(T, \mu)$ is in good agreement with lattice data of the Budapest-Wuppertal and Hot QCD groups. We have also calculated changing in the speed of the sound All this implies the absence of a critical point in the studied range of T and μ_B from the point of view of FCM method.

It should be noted however that we have used both M_D and M_{HL} independent of μ_B in the range $\mu_B < 400$ MeV.

Thank you for your attention!